Earthq Eng & Eng Vib (2009) 8:61-76 **DOI**: 10.1007/s11803-009-9005-8

Numerical modeling of centrifuge cyclic lateral pile load experiments

Nikos Gerolymos[1†], Sandra Escoffier[2‡], George Gazetas[1§] and Jacques Garnier[2‡]

1. *Civil Engineering, National Technical University, Athens, Greece*
2. *Laboratoire Central des Ponts et Chaussées, Nantes, France*

Abstract: To gain insight into the inelastic behavior of piles, the response of a vertical pile embedded in dry sand and subjected to cyclic lateral loading was studied experimentally in centrifuge tests conducted in Laboratoire Central des Ponts et Chaussées. Three types of cyclic loading were applied, two asymmetric and one symmetric with respect to the unloaded pile. An approximately square−root variation of soil stiffness with depth was obtained from indirect in−flight density measurements, laboratory tests on reconstituted samples, and well-established empirical correlations. The tests were simulated using a cyclic nonlinear Winkler spring model, which describes the full range of inelastic phenomena, including separation and re-attachment of the pile from and to the soil. The model consists of three mathematical expressions capable of reproducing a wide variety of monotonic and cyclic experimental *p*−*y* curves. The physical meaning of key model parameters is graphically explained and related to soil behavior. Comparisons with the centrifuge test results demonstrate the general validity of the model and its ability to capture several features of pile−soil interaction, including: soil plastification at an early stage of loading, "pinching" behavior due to the formation of a relaxation zone around the upper part of the pile, and stiffness and strength changes due to cyclic loading. A comparison of the *p*–*y* curves derived from the test results and the proposed model, as well as those from the classical curves of Reese *et al*. (1974) for sand, is also presented.

Keywords: centrifuge test; Winkler model; *p*−*y* curves; cyclic loading; pile-soil separation/gapping; nonlinear response; experimental validation

1 Introduction: empirical and analytical *p*–*y* curves for laterally loaded piles

The response of piles subjected to cyclic lateral loading is governed by the strong nonlinearity of the stress−strain soil behavior that occurs even at low levels of applied load. The problem becomes much more difficult with the appearance of geometric nonlinearities, such as separation of and sliding between pile and soil—phenomena unavoidable under strong excitation.

The methods of lateral pile response analysis are classified into three broad categories:

• limit analysis methods in which the ultimate soil reaction is predetermined from the assumed shape of the pile displacement profile at its ultimate state, i.e., after plastic hinging has transformed the pile into a mechanism (Hansen, 1961; Broms, 1964 a,b).

• Clastic (and inelastic) continuum-based methods which rarely lead to analytical solutions, but are usually materialized through boundary-element, finite-element, or finite-difference type numerical formulations (Banerjee, 1978; Banerjee and Davies, 1978; Poulos and Davis, 1980)

• Linear and nonlinear Winkler spring methods, the most successful of which is the *p*−*y* method (McClelland and Focht, 1958; Matlock, 1970; Reese *et al.*, 1974, 1975; Reese, 1986)

A finite element analysis requires discretization of the pile and the surrounding soil in 3 dimensions (3-D). Equivalent−linear as well as advanced constitutive models based on the theory of plasticity and hypoplasticity have been utilized to reproduce the nonlinear stress−strain soil behavior (Angelides and Roesset, 1981; Trochanis *et al*., 1991; Kimura *et al*., 1995; Wakai *et al*., 1999). However, even today, a 3-D finite element analysis is not a computationally trivial task and is thus infrequently used in engineering practice. Modeling pile−soil separation and gap formation as well as other interface nonlinearities can prove to be especially formidable tasks. Additionally, a 3-D elastoplastic finite-element model would not be easily combined with many structural codes to compute the response of the superstructure.

Correspondence to: Nikos Gerolymos, National Technical University, Athens, Greece
Tel: +30210 772 4075; Fax: +30210 772 2405
E-mail: gerolymos@gmail.com
[†]Lecturer; [‡]Dr.; [§]Professor

Supported by: EU Fifth Framework Program: Environment, Energy and Sustainable Development Research and Technological Development Activity of Generic Nature: The Fight Against Natural and Technological Hazards, Research Project QUAKER Under Contract No. EVG1–CT–2002–00064

Received January 13, 2009; **Accepted** February 5, 2009

In contrast, Winkler-spring modeling is a versatile and economical approach since the analysis of soil-pile interaction is effectively reduced to a one-dimensional problem. It is in essence a semi-empirical method, in which soil resistance is represented by independent springs distributed along the pile. The Winkler-spring model for laterally-loaded piles owes its popularity to the well known semi-empirically derived p–y curves. Obtained on the basis of full-scale experiments, they relate soil reaction (the horizontal result of the soil stresses) with pile deflection at each point of the pile. The main advantages of the p–y method are that it can easily accommodate other experimental results, as necessary; it (indirectly) accounts for soil separation from the pile and sliding at the pile-soil interface; and it can even account for the method of pile installation. The development of p–y curves has been addressed by several researchers (Matlock, 1970; Reese *et al*., 1974; Reese,1986; Yegian and Wright, 1973; Stevens and Audibert, 1979; O' Neill and Murchinson, 1983; Murchinson and O' Neill, 1984; Wu *et al*., 1998; Ashour and Norris, 2000; Kim *et al.,* 2004), and the p–y method constitutes the current state of the art. Its success stems from the fact that even though the p–y curves do not accurately model the soil continuum, they are based on results of field load tests where the continuum is fully satisfied (Reese, 1997).

Note that numerous (mostly successful) attempts have also been published developing cyclic p–y curves for different soils, starting from the conceptual framework of Matlock *et al.* (1978) to the development of the composite centrifuge-based p–y macro-element of Curras *et al*. (1999) and Curras (2000), which consists of viscoelastic, plastic and gap components in series, and can thus model gapping effects, strength degradation, and radiation damping (Boulanger *et al.*, 1999). Similar models were presented by Nogami *et al.* (1992).

Several other approximate nonlinear methods of a different philosophy have also been developed over the years. They are of significant engineering interest, but are beyond the scope of this paper. For more information, refer to Duncan *et al*. (1994), Budhu and Davies (1987) and Kucukarslan and Banerjee (2004) for monotonic loading conditions, and to Tabesh and Poulos (2001) for seismic response, among several other publications. A comprehensive review on the subject was compiled by Pender (1993).

Most of the aforementioned p–y methods employ a semi-empirical approach to developing p–y curves; essentially, the proposed curves are a judicious curve fitting to appropriate full-scale (or centrifuge) experiments. (Judicious meaning with the help of soil mechanics and engineering judgment.)

A different semi-theoretical methodology to developing cyclic p–y curves is *also* possible. One starts with a mathematical model (a p–y "macro-element") and then calibrates its parameters with the help of full-scale and centrifuge experiments, or even with rigorous 3-D numerical results, if available. Validation of the resulting method against other test results would then be necessary before such a method is adopted in practice.

Among a number of such mathematical models proposed over the last twenty years, particularly fruitful has proved the so-called Bouc-Wen model (Bouc, 1971; Wen, 1976). Originally applied to describe inelastic cyclic force-displacement relationships in probabilistic structural dynamics (Baber and Wen, 1981), it was subsequently applied to soil liquefaction analysis as a constitutive τ–γ relationship in simple shear (Pires *et al.*, 1989; Loh *et al.*, 1995) and to the analysis of laterally loaded piles as a monotonic or cyclic p–y relationship (Trochanis *et al.*, 1994; Badoni and Makris, 1995). The latter references are of particular interest in the work presented here, as they showed that a Bouc-Wen model is capable of describing the response of a pile under cyclic and dynamic loading in sufficient engineering detail — at least in cases of "simple" soil conditions.

Recently, Gerolymos and Gazetas (2005 a, b) presented an extension-modification of the original Bouc-Wen model, and they applied it to describe dynamic simple shear τ–γ relationships for wave-propagation site-response analyses and p–y relationships for laterally loaded piles (Gazetas, 2005) and Caissons (2006a, b). Designated as a "BWGG" model, this extended Bouc-Wen model is capable of reproducing complex features of pile-soil interaction, such as: (i) soil *and* pile nonlinearities; (ii) soil-pile interface nonlinearities; (iii) coupling between radiation damping and hysteretic soil response; and (iv) stiffness and strength hardening (or degradation) with cyclic loading. The model was validated against available experimental data. The need, however, for further calibration/validation of the model is unquestionable — hence the work presented in this paper.

The objectives of this paper are: (i) to briefly introduce the key features and some capabilities of the developed BWGG model; (ii) to present the results of cyclic centrifuge experiments on a pile in sand; (iii) to outline the methodology for calibrating the model parameters using the results of one of the tests; and (iv) to apply the method to the other tests and compare them with the centrifuge experiments as well as the "classical" p–y curves of Reese *et al*. (1974). It is hoped that, in the process, some valuable insight into the nature of pile lateral response will be gained.

2 Centrifuge experiments

The centrifuge tests reported here were conducted for the dissertation of Rosquoët (2004) at Laboratoire Central des Ponts et Chaussées [LCPC]; see also Rosquoët *et al.* (2003, 2004). The tests were performed on a single pile subjected to cyclic horizontal loading. The centrifuge models, 1/40 in scale, involved pile head loading with three different force time histories. The experimental set up and the loading time histories (in prototype scale) are shown in Fig 1.

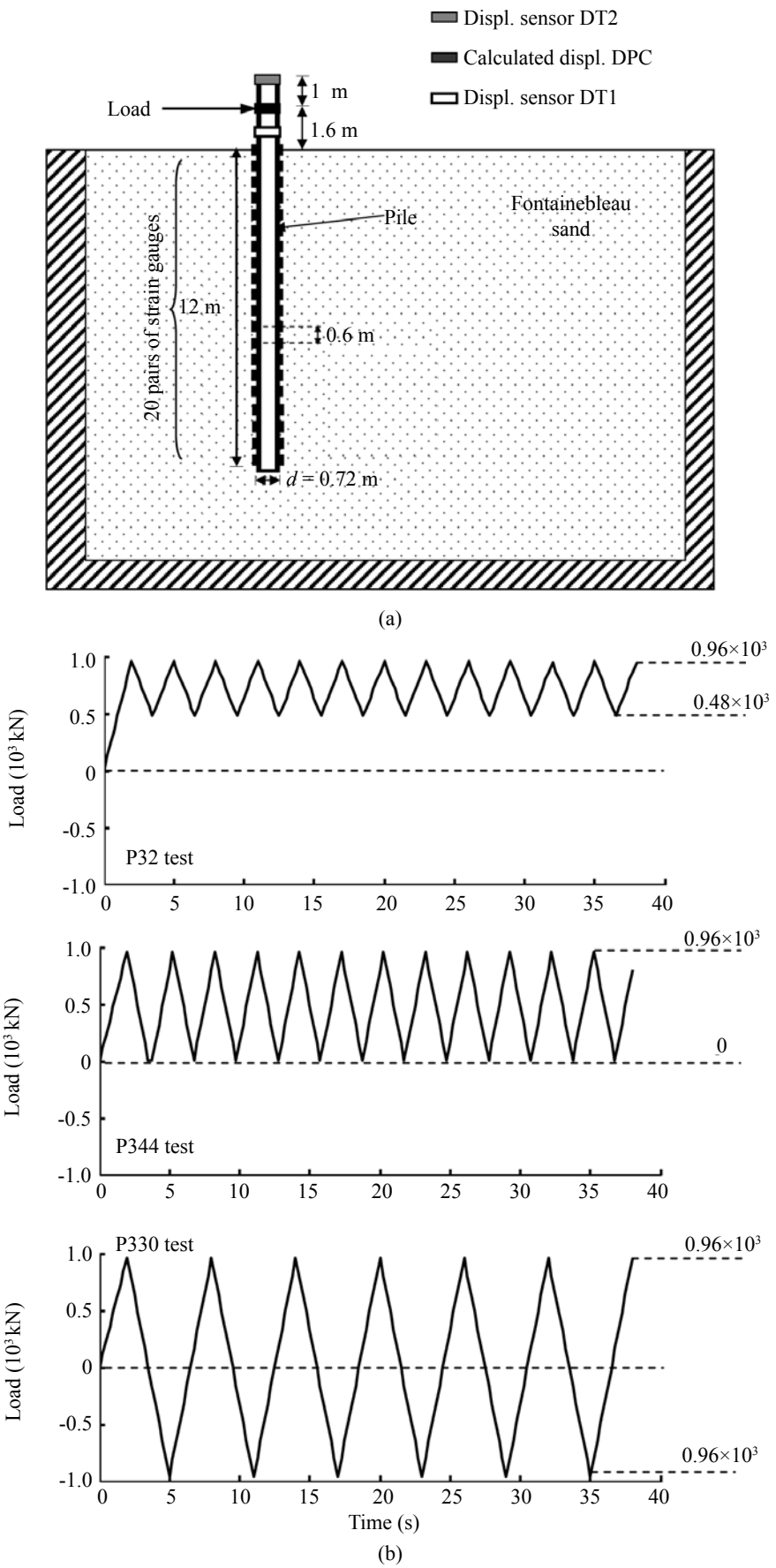

Fig. 1 (a) Experimental setup of the centrifuge tests conducted in LCPC. (b) Load time histories of the three tests (P32, P344 and P330). All dimensions refer to the modeled prototype.

2.1 Centrifuge modeling

It is well known that since soils have stress-dependent stiffness and strength characteristics, the application of N times the gravitational acceleration to a model with length dimensions $1/N$, causes the stresses and mechanical properties of the model to become similar to those of the prototype. Schofield (1980, 1981) and Whitman *et al.* (1981), among several others, have discussed the scaling laws which relate the behavior of a model under static and seismic shaking to the prototype behavior in the field. Over the past decade, dynamic centrifuge techniques have been established as a useful tool for the engineer to investigate the dynamic behavior of geotechnical structures and to calibrate advanced numerical models and procedures.

The centrifuge facility of the LCPC, in Nantes, has a radius of 5.5 m, a maximum model mass of 2000 kg at a centrifuge acceleration of 100 g, and platform dimensions of 1.4 m × 1.15 m. It is currently capable of producing 200 g's of centrifugal acceleration, although of course at a much reduced "payload." The recent acquisition of a servo-hydraulic earthquake actuator has extended the scope of its activities.

2.2 Model description

The presented cyclic lateral load tests were conducted on a vertical friction pile placed in a sand mass of uniform density. The Fontainebleau sand centrifuge "specimens" were prepared by the air sand-raining process into a rectangular container (80 cm wide by 120 cm long by 36 cm deep), with the use of a special automatic hopper developed at LCPC (Garnier, 2002). The desired density of the dry sand was obtained by varying three parameters: (a) the flow of sand (opening of the hopper), (b) the automatically maintained drop height, and (c) the scanning rate. The unit weight and the relative density of the specimen were measured to be $\gamma_d \approx 16.5 \pm 0.04$ kN/m^3 and $D_r = 86\%$ samples, respectively. Laboratory results from (drained and undrained) torsional and direct shear tests on Fontainebleau sand reconstituted specimens indicated mean values of peak and critical-state angles of $\varphi_p = 41.8^o$ and $\varphi_{cv} = 33^o$, respectively. The reader is referred to the official site of the Quaker (2002) research program for details on the aforementioned tests.

The soil properties used for the centrifuge tests are shown in Fig 2, with emphasis on a probable but idealized profile of the shear modulus G_o at small strains. The accuracy of this profile does not have a substantial effect on our numerical results since one of the tests was used to calibrate the model. Evidently, in such relatively-dense sand, the pile used may be considered as flexible (Rosquoet, 2004; Randolph, 1981).

The model pile (scale 1/40) is an aluminium hollow cylinder of 18 mm external diameter, 3 mm wall thickness, and 365 mm length. The flexural stiffness of the pile is 0.197 kN m^2 and the elastic limit stress of the aluminium is 245 kPa. The model and prototype pile characteristics are given in Table 1 (centrifuge tests were carried out at 40 g).

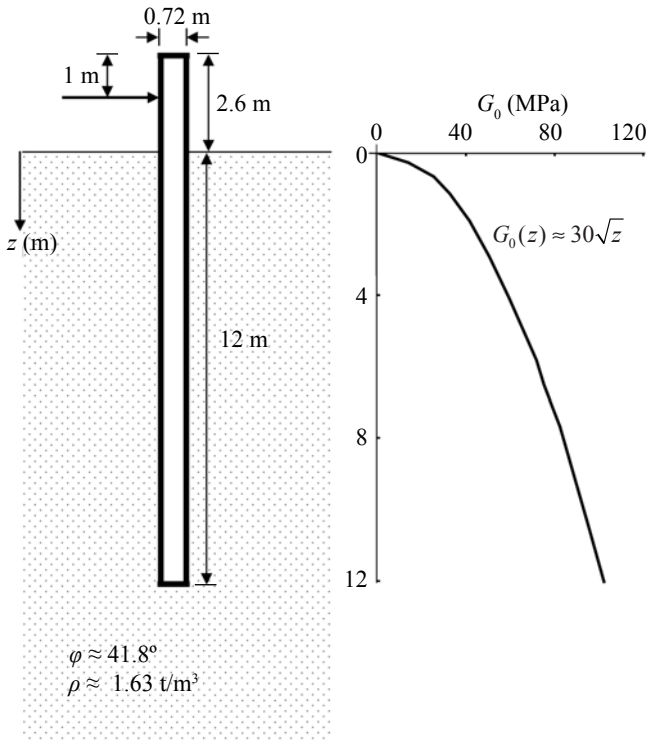

Fig. 2 Pile configuration and soil properties of the three centrifuge tests

Table 1 Pile characteristics

Name	Symbol	Model scale	Prototype scale (40g)
Length	L	38 cm	15.2 m
Depth of pile tip from ground surface	D	30 cm	12 m
External diameter	B	1.8 cm	0.72 m
Internal diameter		1.5 cm	0.6 m
Young's modulus	E	7.4 x 10^4 MPa	
Moment of inertia	I	2.67 x 10^{-9} m^4	6.83 10^{-3} m^4
Bending stiffness	EI	197 N m^2	505 MNm^2
Elastic limit	σ_e	245 MPa	

The instrumentation included two displacement sensors, located at the section of the pile above the ground line, and 20 pairs of strain gauges, positioned along the length of the pile so that the bending moment profile $M(z)$ could be measured during the tests. The resulting earth pressure $p = p(z)$, per unit length along the pile, was obtained by double differentiation of $M(z)$ as established by Matlock and Reese (Reese and Van Impe, 2001). The strain gauges were spaced at 0.6 m (prototype scale) starting from the ground level to the pile tip. This single pile was driven into the sand before rotating the centrifuge (i.e., at 1 g). In flight, the single pile was subjected quasi-statically to horizontal cyclic loading through a servo-jack connected to the pile with a cable. With such a configuration, the pile head is not submitted to any parasitic bending moment.

Three cyclic load tests were performed as shown in Fig. 1 and are discussed later in this paper. The test results were obtained in the form of horizontal force-displacement time histories at the head of the pile, as well as of bending moment, shear force, and soil reaction profiles.

3 Description of the theoretical model: equations and parameters

The BWGG model is a versatile one-dimensional action-reaction relationship, capable of reproducing an almost endless variety of stress-strain or force-displacement or moment-rotation relationships, monotonic as well as cyclic. It is being applied here to model the monotonic and cyclic response of piles, expressing the *p–y* relationship. A simple version of the model is outlined below. More details can be found in Gerolymos and Gazetas (2005 a, b), although the model utilized here is a slightly improved−simplified version of the model in the latter reference.

The constitutive relationship for the lateral soil reaction against a deflecting pile is expressed as the sum of an elastic and a hysteretic component according to:

$$p = \alpha\, k\, y + \left(1-\alpha\right) p_{\mathrm{y}}\, \zeta \qquad (1)$$

where ζ is a dimensionless inelastic parameter expressed in the following differential form:

$$\frac{\mathrm{d}\zeta}{\mathrm{d}y} = \frac{1}{y_0}\left\{1-\left|\zeta\right|^n\left[b+g\,\mathrm{sign}\left(\mathrm{d}y\,\zeta\right)\right]\right\} \qquad (2)$$

p is the result (in the direction of loading) of the normal and shear stresses along the perimeter of a pile segment of unit length; y is the pile deflection at the location of the spring; k is a reference spring stiffness; α is a parameter governing the post yielding stiffness; p_{y} is a characteristic value of the soil reaction related to the initiation of significant inelasticity (yielding); y_0 is a characteristic value of pile deflection related to the initiation of yielding in soil reaction; and n, b and g, are dimensionless quantities that control the shape of the hysteretic soil reaction−pile deflection loop as described below.

Parameter n governs the sharpness of the transition from the linear to the nonlinear range during initial virgin (monotonic) loading. It can take values between 0 and ∞. A large value of n (> 10) models approximately a bilinear hysteretic curve; decreasing n leads to smoother transitions, with plastic behavior occurring at lower loading levels. Parameter α is the ratio of steady-state post yielding to the initial elastic stiffness. The larger the parameter α, the larger the component of the lateral soil reaction resulting from constrained soil dilatancy. When these two parameters, n and α, are properly calibrated, the following can be approximately matched: (a) most lateral *p–y* curves, such as those proposed by Reese *et al*. (1974, 1975) and Matlock (1970), and (b) almost any experimental soil reaction curve. Figures 3 and 4 illustrate the significance of a and n on the resulting *p–y* curves.

Parameters b and g control the unloading-reloading rule. Four basic shapes of hysteresis loops can be generated depending on the relationship between b and g. When $b = g = 0.5$, the stiffness upon reversal equals the initial (maximum) stiffness and, the Masing criterion for loading-uploading-reloading is satisfied. As b tends to 1, the reversal stiffness tends to be equal to the post yielding stiffness right before the reversal point, which implies a strongly nonlinear but near elastic behavior. In the special case where $b = 1$ and $g = 0$, the hysteretic loop degenerates to the monotonic loading curve (nonlinear but elastic behavior). On the contrary, as g tends to 1, the reversal stiffness becomes larger than the initial stiffness (at virgin loading). When $g = 1$ and $b = 0$, the reversal stiffness is two times larger than the initial one. The unloading-reloading parameters b and g can either be constants or variable in the course of cyclic loading. The condition $b + g = 1$ along with $a = 0$ imply a constant ultimate resistance under cyclic loading.

From Equations (1) and (2), the parameter ζ can be eliminated through a straightforward step-by-step numerical integration, which is readily implemented within the framework of codes such as Mathcad and Matlab.

3.1 Modeling separation/gapping of the pile from the soil

A significant issue in pile-soil interaction under cyclic lateral loading is the separation (gapping) of the pile from the soil and the subsequent re-attachment. Separation at the pile-soil interface is implemented in the proposed constitutive law for lateral soil reaction, through the introduction in the differential expression for ζ (Eq. (2)) of a multiplying *"pinching"* function of ζ, h_{p}:

$$h_{\mathrm{p}}\left(\zeta\right) = 1 - \zeta_0 \exp\left[-\left(\frac{y_0\,\zeta}{\delta\,\Delta\left(y\right)}\right)^2\right] \qquad (3)$$

such that Eq. (2) becomes:

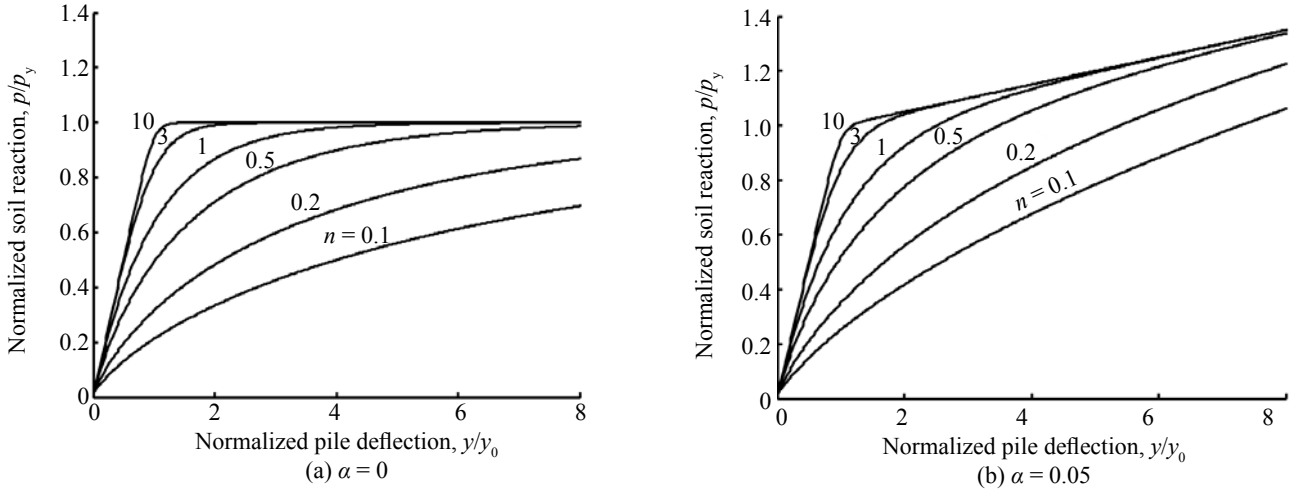

Fig. 3 Normalized soil reaction (p/p_y) versus pile deflection (y/y_0) curves in monotonic loading for selected values of parameter n, derived from the proposed model for $\alpha = 0$ and 0.05

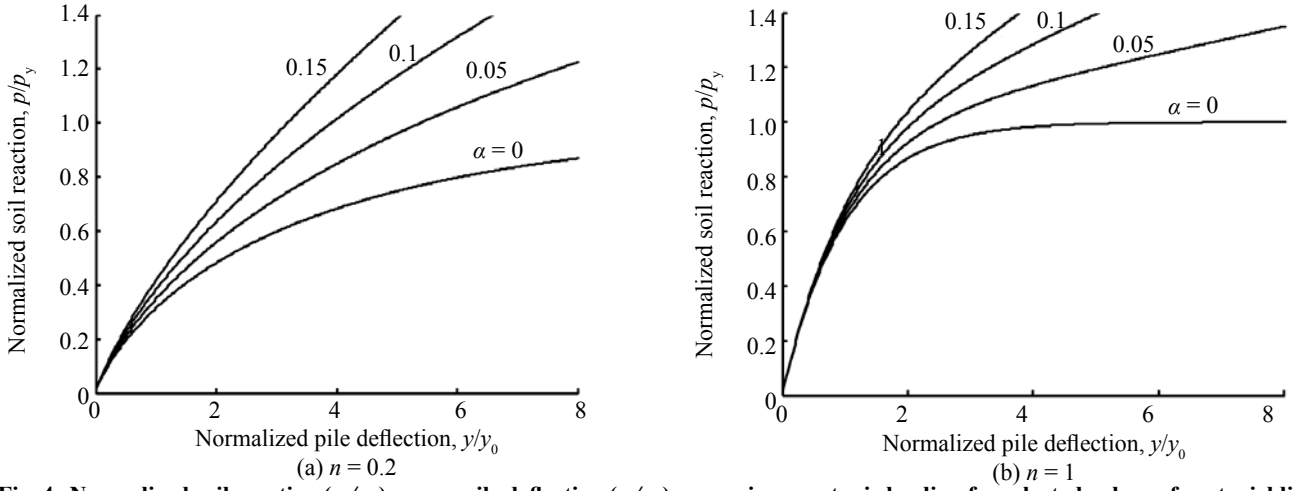

Fig. 4 Normalized soil reaction (p/p_y) versus pile deflection (y/y_0) curves in monotonic loading for selected values of post–yielding parameter α , derived from the proposed model for $n = 0.2$ and 1

$$\frac{\mathrm{d}\zeta}{\mathrm{d}y} = \frac{h_{\mathrm{p}}(\zeta)}{y_0}\left\{1-|\zeta|^n\left[b+g\,\mathrm{sign}(\mathrm{d}y\,\zeta)\right]\right\} \tag{4}$$

In Eq. (3), ζ_0, δ, and Δ are dimensionless parameters that control the gap growth and the sharpness of the transition from the no-contact to the contact region of the lateral soil reaction.

The continuous nature of the pinching function produces smooth hysteresis loops with gradual transition from almost zero stiffness at complete separation to the maximum stiffness when re-attachment occurs. Parameter δ in Eq. (3) controls the gap growth during cyclic (repeated) loading of the pile. Parameter ζ_0, determines the "drag" (i.e. side shear) resistance within the gap. It takes values between 0 and 1, with the drag resistance becoming negligible (sharp separation) when ζ_0 approaches 1. In case of a stiff cohesive soil, a value of $\zeta_0 \approx 1$ could be adopted if loading in two directions generates a complete gap around the pile (sharp separation, negligible drag forces). On the other hand, when the pile is embedded in a cohesionless soil, the formation of a relaxation zone around the pile is the most possible local failure mechanism near the ground surface (diffuse failure), rather than the opening of a clear gap (as in a cohesive soil). In that case, values of $\zeta_0 < 1$ close to 0 should be used.

Parameter $\Delta = \Delta(y)$ is the maximum attained displacement when y is positive, or the minimum attained displacement when y is negative.

A simplified but reasonable hypothesis is that separation takes place when the net tensile stress at a point of pile-soil interface becomes larger than the product of the difference between the earth pressure at rest σ'_{h0} and the lateral active earth pressure σ'_{ha}, multiplied by the pile diameter d, i.e.:

$$\left(\sigma'_{\mathrm{h0}} - \sigma'_{\mathrm{ha}}\right) d < p \tag{5}$$

Figure 6 portrays lateral soil reaction versus pile

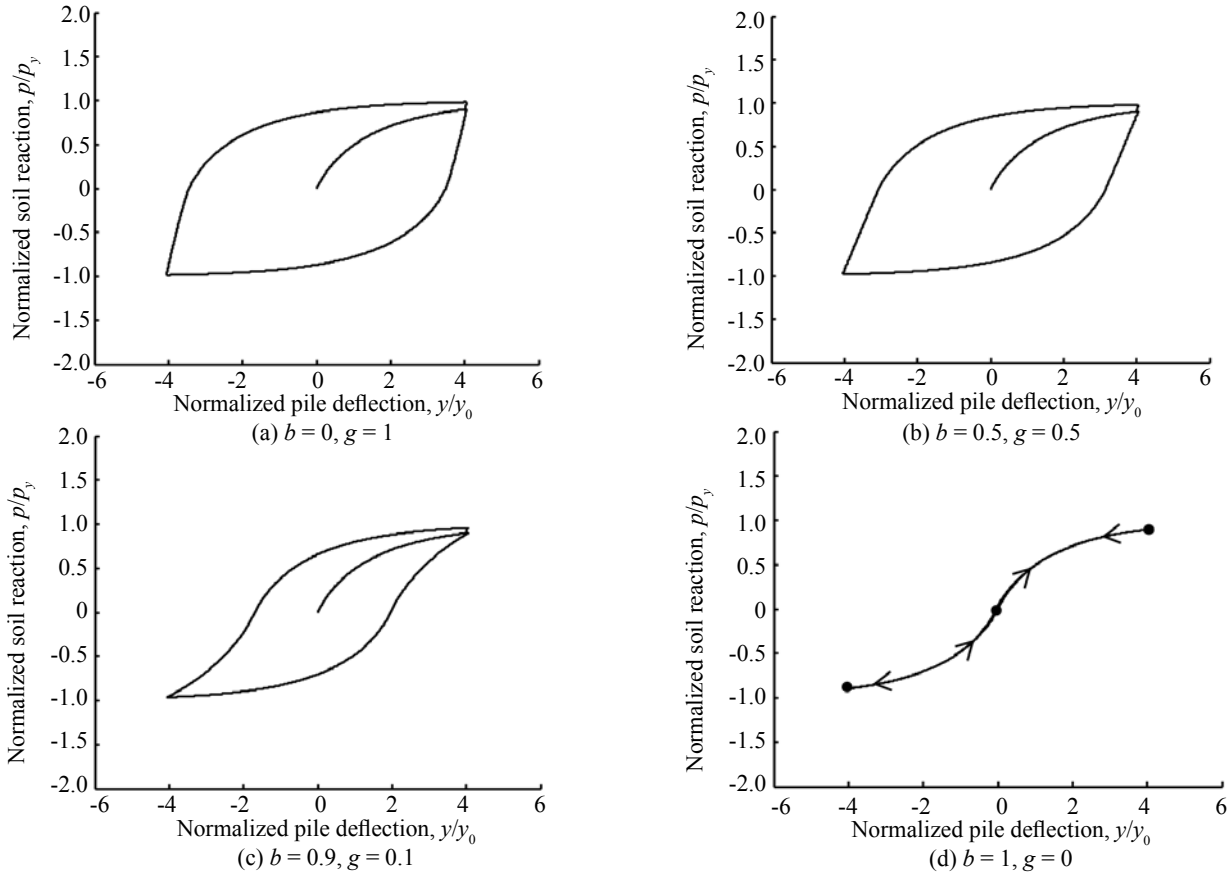

Fig. 5 Normalized hysteresis loops of soil reaction versus pile deflection for $n = 1$ and different values of b and g. The Masing criterion for unloading–reloading is recovered for $b = 0.5$, $g = 0.5$.

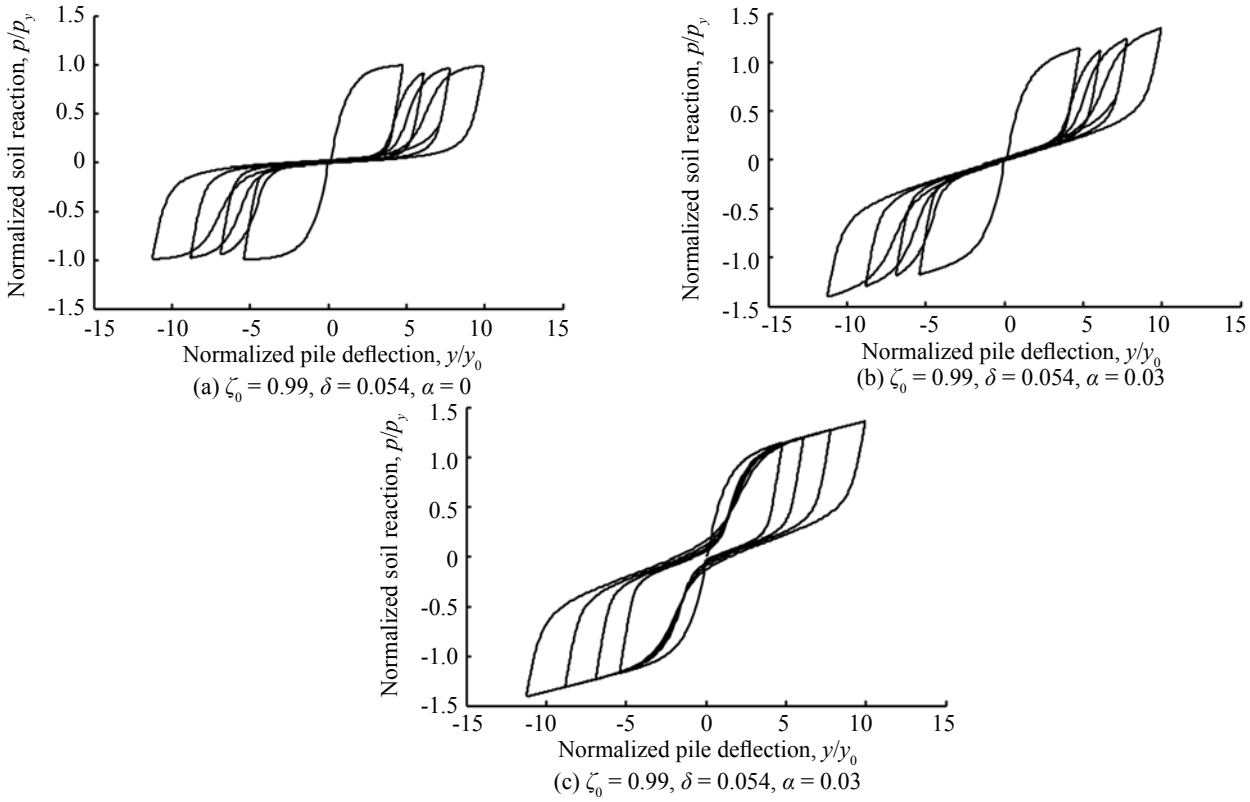

Fig. 6 Normalized hysteresis loops of soil reaction versus pile deflection, including separation of the pile from the soil derived from Eq.s (2), (3), and (6): (a) No drag force and no strength hardening develop during separation ($n = 1$, $b = 0.5$, $\alpha = 0$, $\zeta_0 = 0.99$, and $\delta = 0.054$); (b) Substantial strength hardening but no drag force develop during separation ($n = 1$, $b = 0.5$, $\alpha = 0.03$, $\zeta_0 = 0.99$, and $\delta = 0.054$); and (c) drag force of the order of 10% of the ultimate soil reaction and significant strength hardening develop during separation ($n = 1$, $b = 0.5$, $\alpha = 0.03$, $\zeta_0 = 0.97$, and $\delta = 0.054$)

deflection hysteresis loops with gapping effect, for different values of parameters ζ_0 and δ. Evidently, the model can reproduce a variety of situations in which gapping dominates.

3.2 Stiffness and strength parameters for cohesionless soil

The following expression for the small-amplitude stiffness k (= p_y / y_0) in Eq. (1) is adequate:

$$k = 1.2\ E_s \tag{6}$$

where E_s is the Young's modulus of the soil (Gazetas and Dobry,1984). Note that k has units of stiffness per unit length of the pile, corresponding to the traditional "subgrade modulus" (in units of pressure per unit length) multiplied by the diameter d of the pile. Eq. (6) has been derived by matching the dynamic head displacement of the Winkler model with the one computed through finite element analyses of a soil with Poisson's ratio ν = 0.4. Other expressions for the subgrade modulus could also be used in other cases, such as those by Matlock and Reese (in the aforesaid publications) from the scaled field tests.

In case of a pile embedded in cohesionless soil, the strength parameter p_y in Eq. (1) can be calculated through the analytical expression of Broms (1964) for the ultimate soil reaction:

$$p_y = 3\sigma'_v \tan^2\left(45^\circ + \frac{\phi}{2}\right) d \tag{7}$$

in which σ'_v is the effective vertical stress and φ is the friction angle of the soil. Eq. (7) is very often preferred in practice from other more rigorous expressions for its simplicity and sufficient engineering accuracy, in view of its accord with experimental and numerical results. It is used in all the subsequent analyses as well.

3.3 Numerical formulation for pile–soil system

With the constitutive model for lateral soil reaction developed in the previous sections, the pile-soil interaction problem under cyclic lateral loading reduces to the analysis of a beam supported on a nonlinear Winkler foundation. Equilibrium of the pile gives:

$$\frac{\partial^2}{\partial z^2}\left(E_p I_p \frac{\partial^2 y(z,t)}{\partial z^2}\right) + p(z,t) = 0 \tag{8}$$

where E_p and I_p are the pile modulus of elasticity and cross-sectional moment of inertia, respectively. Equation (9) forms a system of (coupled) ordinary and differential equations with Eqs. (1), (3), and (4). An explicit finite-difference scheme is used for the solution of this system, with the possibility of considering the variation of pile and soil properties along the pile length. Head and tip boundary conditions are properly taken into account.

The proposed model for piles is next applied to simulate the pile response in the centrifuge cyclic lateral load tests described in the beginning.

4 Numerical simulation of the centrifuge tests

The proposed model is first calibrated against the results of one of the tests (designated as P32). Subsequently, it is applied to predict the measured data of the other two tests (P330 and P344). The three tests differ by the characteristics of the cyclic loading sequences as shown in Fig. 1 (one-way and two-way loading at different load amplitudes). It should be noted that the applied loads always stay in the domain of service loads. The maximum applied load of 960 kN is indeed just about one third of the maximum lateral resistance of the pile (Rosquoet, 2004; Broms, 1964a, b).

The bending moment distribution with depth $M(z)$, obtained from the bending strains measured during each test through the strain gauges, were utilized to calculate the shear force, $Q(z)$, and soil reaction, $p(z)$, diagram:

$$Q(z) = \frac{\mathrm{d}M(z)}{\mathrm{d}z} \tag{9a}$$

and

$$p(z) = \frac{\mathrm{d}^2 M(z)}{\mathrm{d}z^2} \tag{9b}$$

High-order spline functions which interpolate between two successive pairs of experimental points (M_i, z_i) and (M_{i+1}, z_{i+1}) were utilized to this end. The experimental $M = M(z)$ curves were also integrated twice to get the pile deflection diagram $y = y(z)$ and the boundary conditions (head and tip pile displacement) were used to determine the needed two constants.

4.1 Calibration of model parameters against test P32; comparison with empirical p–y curves

The calibration of the model parameters was based on matching the calculated with the recorded force-displacement curve at the pile head (calculated displacement DPC in Fig 1). Only density measurements were performed and Hardin's (1978) formula was applied to evaluate the soil shear modulus at low-amplitude strains:

$$G_0 = \frac{S\sqrt{(1+2K_0)\ p_a\ \sigma'_v}}{2\sqrt{3}\,(1+\nu)\left(0.3+0.7\,e_0^2\right)} \tag{10}$$

in which the stiffness coefficient S varies in the range of 1200 and 1500 for clean sands, K_0 is the coefficient of earth pressure at rest, e_0 is the initial void ratio, and p_a is the atmospheric pressure. For $e_0 \approx 0.59$, and assuming K_0 = 0.5, ν = 0.4, and S = 1400, the maximum shear modulus at the effective stress level of 0.1 MPa is approximately equal to 75 MPa. The distribution of G_0 with depth is

shown in Fig. 2. The initial subgrade modulus of the nonlinear Winkler springs is calculated from Eq. (6), whereas Brom's formula [Eq. (7)] is utilized to estimate the ultimate soil reaction. The unloading-reloading parameter b is taken to be equal to 0.50.

A trial-and-error method was used to adjust the values of the pinching parameters ζ_0 and δ, and the monotonic loading parameters n and α. The following combination was found to give the best results: (a) n = 0.05 and α = 0.03 for monotonic loading; and (b) n = 0.15 and α = 0.025 for cyclic loading. The pinching parameters were calculated as ζ_0 = 0.95 and δ = 0.054. Note that the parameter n is not kept constant; its initial value of 0.05 changes to 0.15 after the first reversal in the loading history, reflecting the stiffness hardening of the pile response under cyclic loading due to densification of the sand.

Figure 7(a) compares the p–y curves at depths of 6 m, 3.6 m, and 1.8 m computed with the proposed model to those of Reese (1974) for the particular sand. The calculation of the p–y curves is based on the best fitting of: the P32 test, and (b) Reese's curves. In order for the p–y curves to be in a comparable form, Eq. (6) for the initial subgrade modulus of the spring and Eq. (7) for the ultimate lateral soil reaction, have also been implemented for calculation of slightly modified Reese curves. It is interesting to note that the inelastic component of the lateral soil reaction is underestimated with Reese's curves, while the initial stiffness is overestimated. Different p–y curves would result from the proposed model if a direct fitting onto Reese's p–y curves is performed. Such fitting is shown in Fig 7(b), only for comparison purposes.

Figure 8 shows the comparison between measured

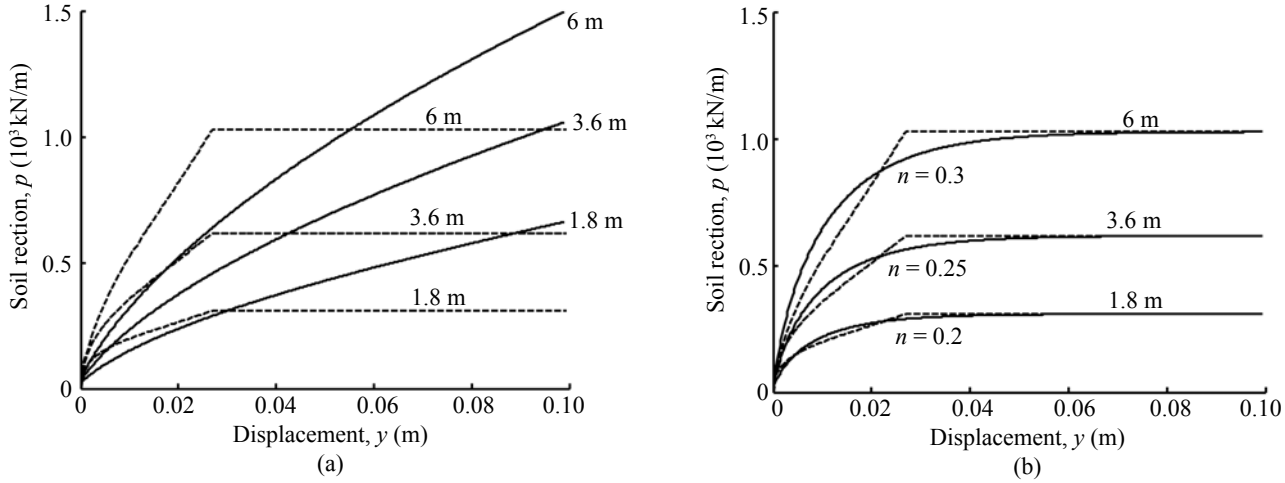

Fig. 7 (a) Comparison of the p–y curves at three different depths derived with the proposed model (solid lines) after calibration with test P32, and those developed by Reese & Matlock for sand (dashed lines). Based on best fitting the recorded force-displacement curve at sensor DPC. (Derived model parameter values: n = 0.05, α = 0.03). (b) Comparison of the p–y curves at the same three depths derived with the proposed model (solid lines) by fitting Reese's (1974) curves. (Derived model parameter values: n = 0.2–0.3, α = 0)

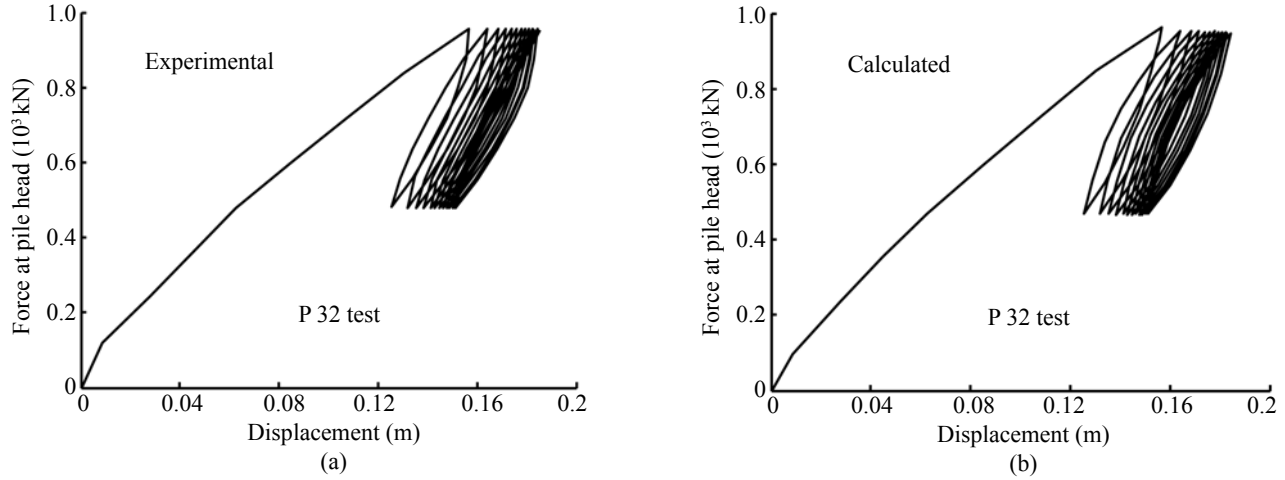

Fig. 8 (a) Experimental and (b) computed total force-displacement curve at sensor DPC for test P32 which was utilized in the calibration

and computed (from the calibrated model) force-displacement curve at the head of the pile. The good agreement attests only to the capability of this model to reproduce the cyclic *p–y* curves. Figures 9 and 10 compare computed versus recorded bending moment, shear force, and soil reaction profiles at different stages of loading. The success of this comparison is an indication of proper calibration of the model against this centrifuge test; it is encouraging only in view of the well known difficulty to simultaneously match detailed force-displacement time history, internal pile forces, and soil reaction profiles.

4.2 Comparison of numerical results with two cyclic experiments

The calibrated model (from the P32 test) is utilized to predict the results of the P344 test (cyclic loading without sign reversal) and the P330 test (fully cyclic loading with sign reversal).

4.2.1 Test P344: asymmetric cyclic force ranging from 960 to 0 kN

The computed force-displacement curve at the pile head is compared to the experimental data from the P344 test in Fig. 11. The comparison of the predicted

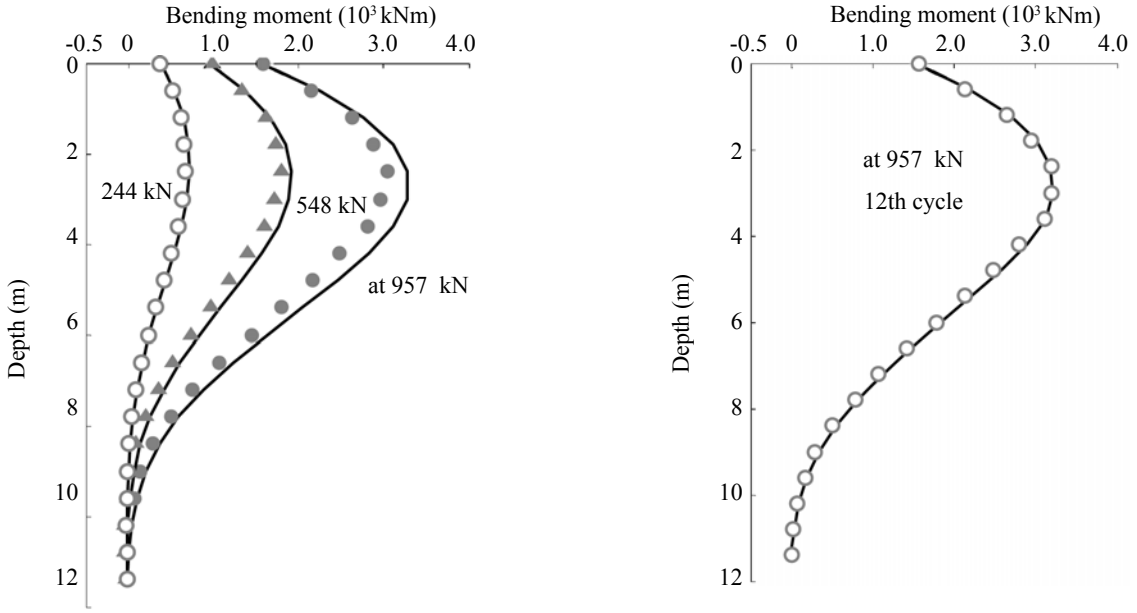

Fig. 9 Comparison of computed (solid lines) and recorded (circles and triangles) bending moment distributions at different stages of loading, for test P32 which was utilized in the calibration

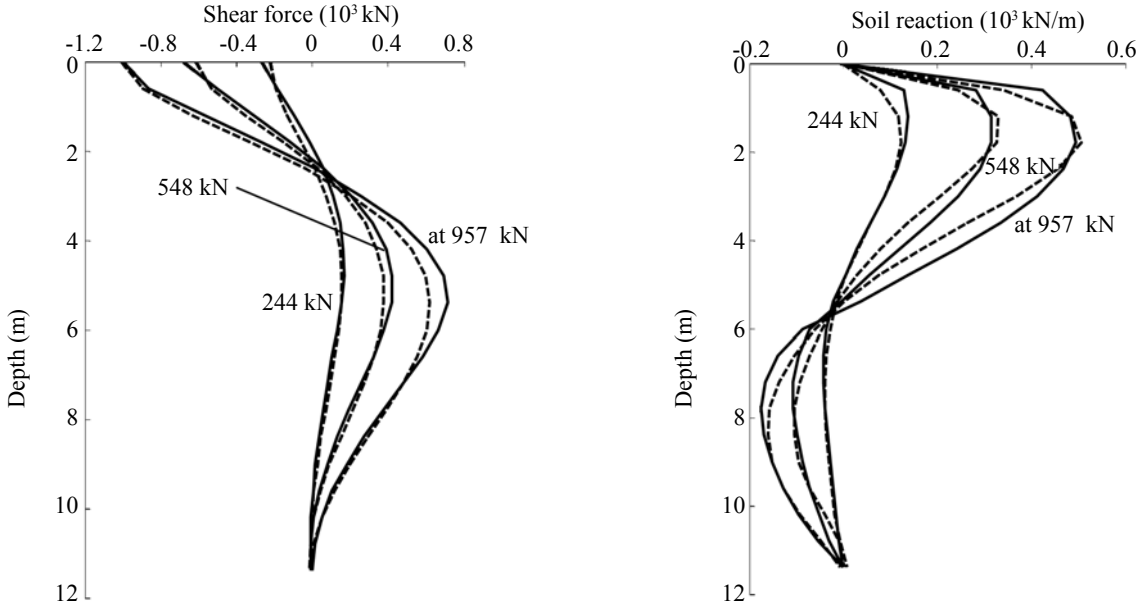

Fig. 10 Comparison of computed (solid lines) and obtained from spline interpolation and differentiation of the *M-z* experimental data (dashed lines) shear force and soil reaction distributions at different stages of loading, for test P32 which was utilized in the calibration

to the measured bending moment, shear force, and soil reaction distributions with depth is presented in Figs 12 and 13 for various stages of loading

The agreement between measurements and computations is in general quite satisfactory for the force-displacement curve at the pile head, as well as for the bending moment and shear force diagrams with depth. The model is capable of reproducing:

(a) the highly nonlinear soil behavior even at low loading levels,

(b) the stiffer reversal stiffness of the pile response compared to the virgin loading (initial) stiffness, and

(c) the strength relaxation of the pile response with cyclic loading. The displacement at which the maximum applied external force occurs, increases with increasing cycle number.

The shapes of hysteresis loops, although not in very good agreement with the experimental curves, reveal the beginning of a pinching behavior — apparently the result of pile-soil separation and re-attachment near the top.

Some differences are also noted between computed and measured soil reaction profiles. More specifically, the maximum soil reaction is underestimated by the proposed model, whereas soil yielding at greater depths is overestimated. This discrepancy may be attributed to several factors, including: (a) the approximate nature of the G_o profile which, after all, was not obtained from direct in-flight measurements, and (b) the conservatism in Brom's formula for ultimate soil reaction (Eq. (7)).

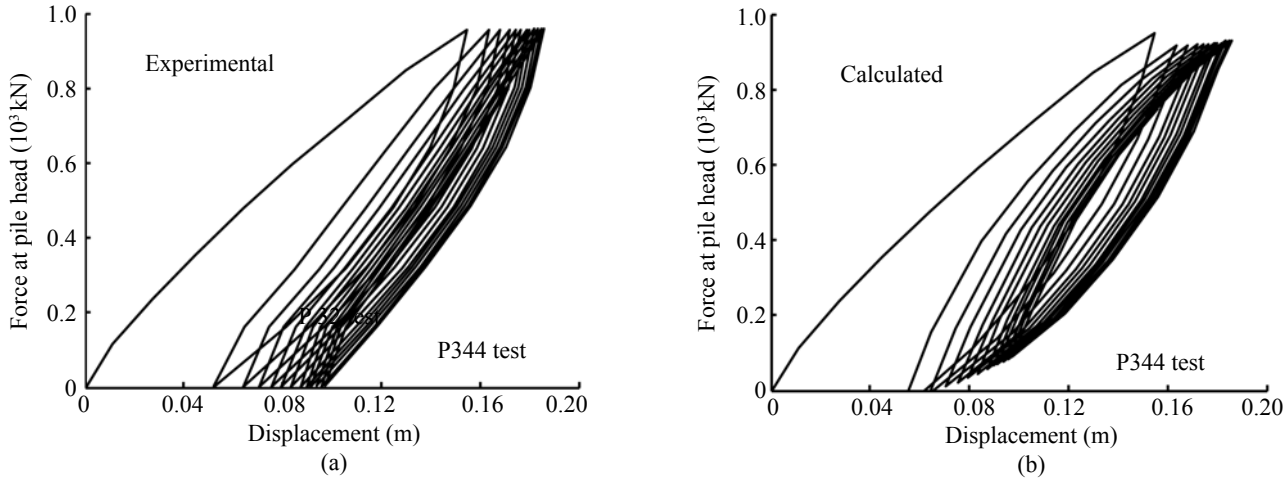

Fig. 11 (a) Experimental and (b) computed force-displacement curve at sensor DPC for the independent-of-calibration test P344 (asymmetric cyclic force, ranging between 960 kN and 0 kN)

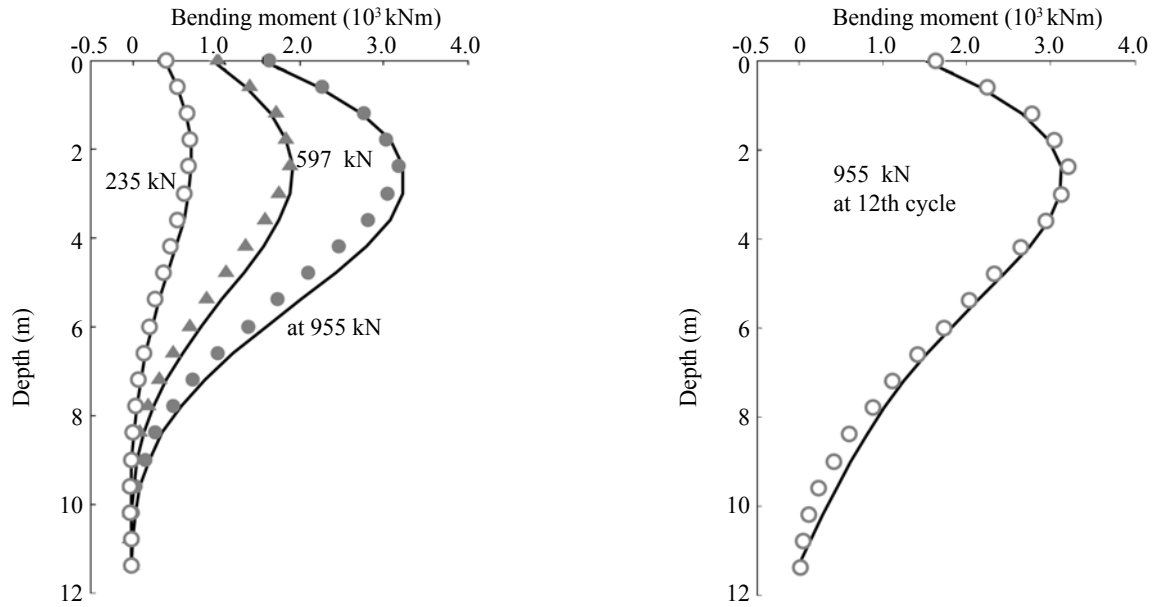

Fig. 12 Comparison of computed (solid lines) and recorded (circles and triangles) bending moment distributions at different stages of loading, for test P344 (asymmetric cyclic force, ranging between 960 kN and 0 kN)

Nevertheless, it is very good that the model captures the downward "migration" of the maximum soil reaction with increasing loading intensity — apparently the result of progressively increasing depth of soil yielding near the top.

4.2.2 Test P330: symmetric cyclic force ranging between ± 960 kN

Similarly satisfactory are the comparisons between theoretical predictions and the results of the P330 test presented in Figs 14, 15 and 16. Specifically, it is seen that the model adequately predicts the following detailed trends:

(a) the stiffness hardening of the pile under cyclic loading, possibly due to densification of the sand in the vicinity of the pile. (Notice that the secant stiffness increases slightly with increasing number of cycles.)

(b) the narrowing of the force-displacement hysteretic loop, which could possibly be attributed to the beginning of formation of a relaxation zone (gapping) around the pile and near the ground surface.

Note also that the maximum bending moment is slightly underpredicted, whereas the soil reaction with depth is better captured than in the P344 test.

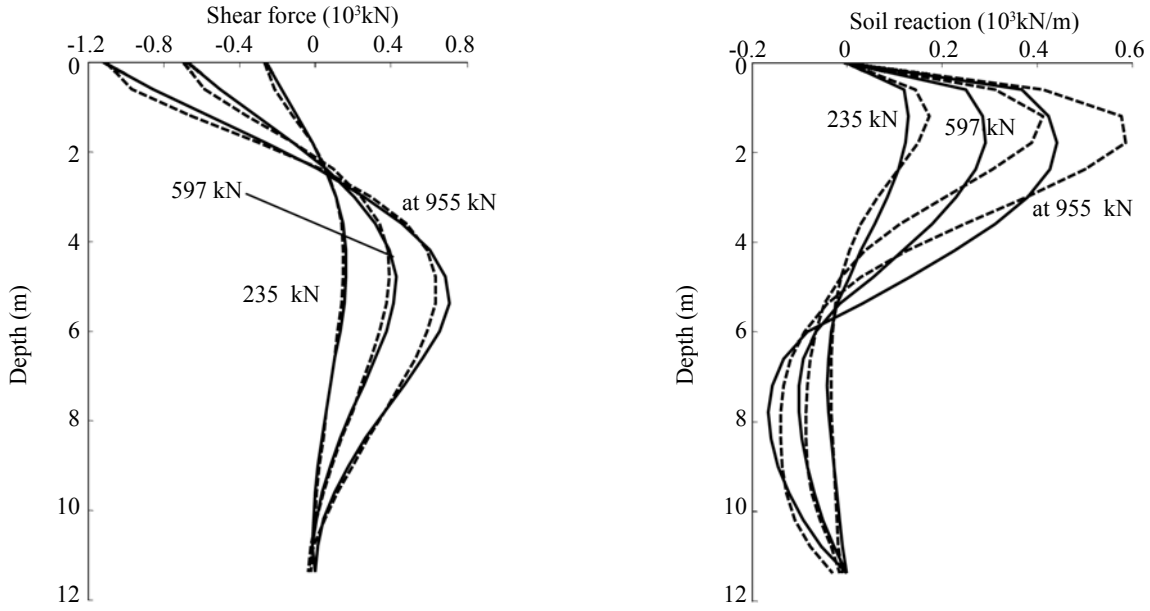

Fig. 13 Comparison of computed (solid lines) and obtained from spline interpolation and differentiation of the M–z experimental data (dashed lines) shear force and soil reaction distributions at different stages of loading, for test P344 (asymmetric cyclic force, ranging between 960 kN and 0 kN)

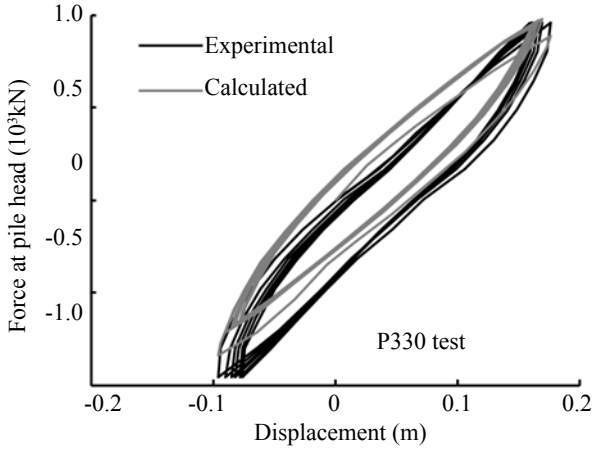

Fig. 14 Comparison of computed (gray solid line) and experimental (black solid line) force-displacement curve at sensor DPC for test P330 (symmetric cyclic force, ranging between 960 kN and −960 kN)

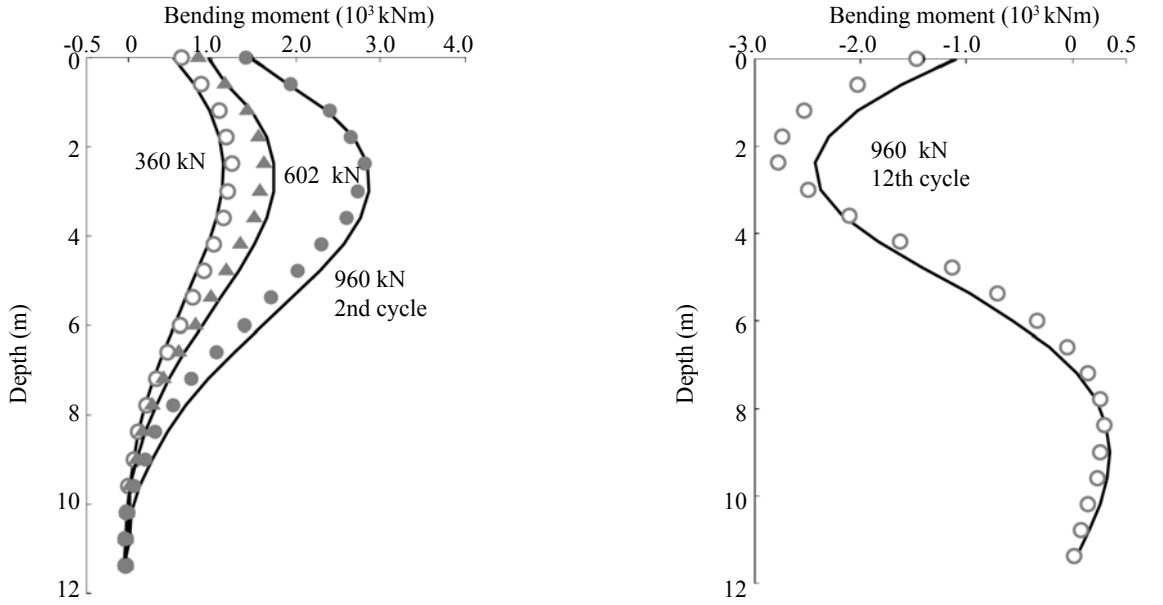

Fig. 15 Comparison of computed (solid lines) and recorded (circles and triangles) bending moment distributions at different stages of loading, for test P330 (symmetric cyclic force, ranging between 960 kN and −960 kN)

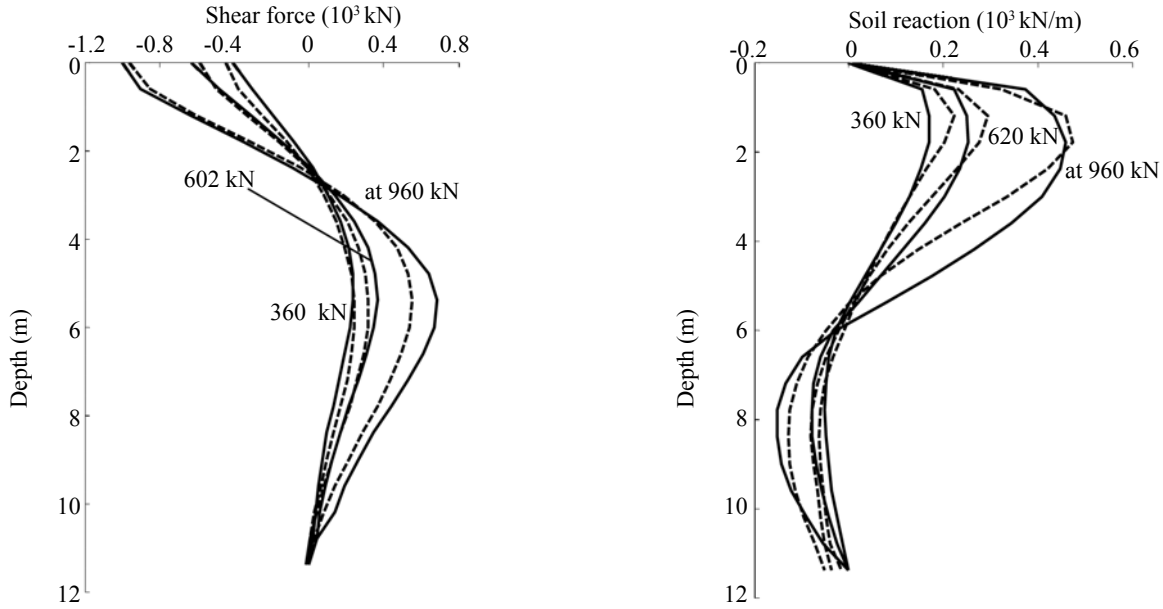

Fig. 16 Comparison of computed (solid lines) and obtained from spline interpolation and differentiation of the M–z experimental data (dashed lines) shear force and soil reaction distributions at different stages of loading, for test P330 (symmetric cyclic force, ranging between 960 kN and −960 kN)

5 Conclusions

A nonlinear Winkler model is applied to obtain the response of a vertical pile subjected to cyclic lateral loading during three centrifuge tests conducted at LCPC, Nantes. A new soil reaction-displacement (p–y) relationship is utilized to model the soil reaction, including separation and gapping of the pile from the soil. The model parameters are related to physical soil properties. Calibrated to match the results of one centrifuge test, the model is subsequently utilized to predict the recorded data of two other tests. A comparison is given between the calculated p–y curves and those proposed by Reese (1974). The model adequately reproduces the soil yielding that occurs even at very low loading levels. The bending moment and shear force distribution with depth are predicted very well, whereas there is a small discrepancy between computed

and measured soil reactions. Finally, the model is shown to be capable of predicting some complicated features of the experimental results arising from counteracting phenomena such as strength relaxation and stiffness hardening of the pile with cyclic loading, as well as the reduction in hysteretic damping due to the development of a relaxation zone around the upper part of the pile.

The maximum lateral load applied in the studied tests was in all cases only 1/3 of P_{ult}. The next phase of this research program will feature loads up to 80% of $P_{ult.}$ At such intense loading, the nonlinear phenomena described in this paper will dominate the pile response; and they will provide an extreme test for the proposed method.

Acknowledgments

The analytical and part of the experimental work of this paper have been conducted with financial support from the EU Fifth Framework Program: Environment, Energy and Sustainable Development Research and Technological Development Activity of Generic Nature: The fight against Natural and Technological Hazards, Research Project QUAKER, Contract number: EVG1–CT–2002–00064. Dr. V. Georgiannou, of the National Technical University of Athens, performed some of the laboratory tests on Fontainebleau sand utilized in our study.

References

Angelides DC and Roesset JM (1981), "Nonlinear Lateral Dynamic Stiffness of Piles," *Journal of the Geotechnical Engineering Division*, ASCE, **107**(11): 1443−1459.

Ashour M and Norris G (2000), "Modelling Lateral Soil -pile Response Based on Soil-pile Interaction," *Journal of Geotechnical Geoenvironmental Engineering,* ASCE, **126**(5): 420–428.

Baber TT and Wen YK (1981), "Random Vibration of Hysteretic Degrading Systems," *Journal of Engineering Mechanics*, ASCE, **107**: 1069−1087.

Badoni D and Makris N (1995), "Nonlinear Response of Single Piles Under Lateral Inertial and Seismic Loads," *Soil Dynamics and Earthquake Engineering*, **15**: 29−43.

Banerjee PK (1978), "Analysis of Axially and Laterally Loaded Pile Groups," *Developments in Soil Mechanics*, London: Applied Science Publishers, 317−346.

Banerjee PK and Davies TG (1978), "The Behavior of Axially and Laterally Loaded Piles Embedded in Nonhomogeneous Soils", *Geotechnique*, **28**(3): 309−326.

Bouc R (1971), "Modele Mathematique d' Hysteresis," *Acustica,* **21**: 16−25.

Boulanger RW, Curras CJ, Kutter BL, Wilson DW and Abhari A (1999), "Seismic Soil-pile-structure Experiments and Analyses," *Journal of Geotechnical and Geoenvironmental Engineering*, ASCE, **125**(9): 750−759.

Broms BB (1964a), "Lateral Resistance of Piles in Cohesive Soils," *Journal of Soil Mechanics and Foundations Division*, ASCE, 1964, **90**: SM2, 27-63.

Broms BB (1964b), "Lateral Resistance of Piles in Cohesionless Soils," *Journal of Soil Mechanics and Foundations Division,* ASCE, 1964, **90**: SM3, 123-56.

Budhu M and Davies TG (1987), "Nonlinear Analysis of Laterally Loaded Piles in Cohesionless Soils," *Canadian Geotechnical Journal*, **24:** 289−296.

Curras CJ (2000), "Seismic Soil-pile-interaction for Bridge and Viaduct Structures," *Ph.D. Dissertation*, University of California, Davis.

Curras CJ, Boulanger RW, Kutter BL and Wilson DW (1999), "Seismic Soil-pile-structure Interaction in Soft-clay," *Proceedings of the 2nd International Conference on Earthquake Geotechnical Engineering,* P.Seco Pinto (ed.), Published by A.A. Balkema, Rotterdam.

Duncan JM, Evans LT, Jr. and Ooi PSK (1994), "Lateral Load Analysis of Single Piles and Drilled Shafts," *Journal of the Geotechnical Engineering Division*, ASCE, **120**(5): 1018−1033.

Garnier J (2002), "Properties of Soil Samples Used in Centrifuge Models," *Invited Keynote Lecture, International Conference on Physical Modelling in Geotechnics – ICPMG '02*, R. Phillips *et al*. (eds), Published by A.A. Balkema, Rotterdam, **1**: 5−19.

Gazetas G and Dobry R (1984), "Horizontal Response of Piles in Layered Soils", *Journal of Engineering Mechanics,* ASCE, **110**, 20−40.

Gerolymos N and Gazetas G (2005a), "Constitutive Model for 1−D Cyclic Soil Behavior Applied to Seismic Analysis of Layered Deposits," *Soils and Foundations*, **45**(3): 147−159.

Gerolymos N and Gazetas G (2005b), "Phenomenological Model Applied to Inelastic Response of Soil-pile Interaction Systems," *Soils and Foundations*, **45**(4): 119−132.

Gerolymos N and Gazetas G (2006a), "Development of Winkler Model for Static and Dynamic Response of Caisson Foundations with Soil and Interface Nonlinearities", *Soil Dynamic and Earthquake Engineering*, **26**(5): 363−376.

Gerolymos N and Gazetas G (2006b), "Static and Dynamic Response of Massive Caisson Foundations with Soil and Interface Nonlinearities — Validation and Results", *Soil Dynamics and Earthquake Engineering,* **26**(5): 377−394

Hansen BJ (1961), "The Ultimate Resistance of Rigid Piles Against Transversal Forces," *The Danish Geotechnical Institute Bulletin*, **12**: 5−9.

Hardin BO (1978), "Nature of Stress-strain Behavior for Soils," *Proceedings of the Specialty Conference on Earthquake Engineering and Soil Dynamics*, ASCE, **1**: 3–90.

Kim BT, Kim NK, Lee WJ and Kim YS (2004), "Experimental Load-transfer Curves for Laterally Loaded Piles in Nak-dong River Sand," *Journal of Geotechnical and Geoenvironmental Engineering,* ASCE, **130**(4): 416−425.

Kimura M, Adachi T, Kamei H and Zhang F (1995),

"3-D Finite Element Analyses of the Ultimate Behavior of Laterally Loaded Cast-in-place Concrete Piles," *Proc. 15th Int. Symp. on Numerical Models in Geomechanic.,* Davos, Switzerland, 589−594.

Kucukarslan S and Banerjee PK (2004), "Inelastic Analysis of Pile-soil Interaction," *Journal of Geotechnical and Geoenvironmental Engineering*, ASCE, **130**(11): 1152−1157.

Loh CH, Cheng CR and Wen YK (1995), " Probabilistic Evaluation of Liquefaction Potential Under Earthquake Loading," *Soil Dynamics and Earthquake Engineering*, **14:** 269−278.

Matlock H (1970), "Correlations for Design of Laterally Loaded Piles in Soft Clay," *Proceedings*, *Second Annual Offshore Technology Conference*, Houston, Texas, **1**: Paper No. OTC 1204, 577−594.

Matlock H, Foo SHC and Bryant LM (1978): "Simulation of Lateral Pile Behavior Under Earthquake Motion," *Earthquake Engineering and Soil Dynamics*, ASCE, **II**: 600−619.

McClelland B and Focht JA, Jr. (1958), "Soil Modulus for Laterally-loaded Piles," *Transaction of ASCE*, **123:** 1049−1086

Murchison JM and O' Neil MW (1984), "Evaluation of *p–y* Relationships in Cohessionless Soil," *Analysis and design of pile foundations*, ASCE, New York, 174-191.

Nogami T, Otani J, Konagai K and Chen HI (1992), "Nonlinear Soil-pile Interaction Model for Dynamic Lateral Motion," *Journal of Geotechnical Engineering,* ASCE, **118**(1): 89−106.

O' Neil MW and Murchison JM (1983), "An Evaluation of *p–y* Relationships in Sand," *Report of the American Petroleum Institute*, Washington, D.C.

Pender MJ (1993), "A Seismic Pile Foundation Design Analysis," *Bulletin of the New Zealand National Society for Earthquake Engineering,* **26**(1): 49−160

Pires JA, Ang AHS and Katayama I (1989), "Probalistic Analysis of Liquefaction," *Proceedings of 4th International Conference on Soil Dynamics and Earthquake Engineering,* Mexico, 1989.

Poulos HG and Davis EH (1980), *Pile Foundation Analysis and Design,* John Wiley & Sons.

Quaker (2002), Fault-rupture and Strong Shaking Effects on the Safety of Composite Foundations and Pipeline Systems: http://www.dundee.ac.uk/civileng/quaker.

Randolph MF (1981), "The Response of Flexible Piles to Lateral Loading," *Geotechnique,* **31**(2): 247−259.

Reese LC (1986), "Behavior of Piles and Pile Groups Under Lateral Load," *Federal Highway Administration Report FHWA/RD−85/106*, Washington D.C.

Reese LC (1997), "Analysis of Laterally Loaded Piles in Weak Rock," *Journal of Geotechnical and Geoenvironmental Engineering,* ASCE, **123**(11): 1010−1017.

Reese LC, Cox WR and Koop FD (1974), "Analysis of Laterally Loaded Piles in Sand," *Proceedings*, *Fifth Annual Offshore Technology Conference*, Paper No. OTC 2080, Houston, Texas, 1974, **II**: 473-485.

Reese LC, Cox WR and Koop FD (1975), "Field Testing and Analysis of Laterally Loaded Piles in Stiff Clay," *Proceedings*, *Seventh Offshore Technology Conference*, Paper No. OTC 2312, Houston, Texas, **II**, 672−690.

Reese LC and Van Impe WF (2001), *Single Piles and Pile Groups under Lateral Loading*, A.A. Balkema.

Rosquoët F (2004), Pieux Sous Charge Latérale Cyclique, Thèse de doctorat de l'Ecole Centrale de Nantes et de l'Université de Nantes, 305p.

Rosquoët F, Canepa Y, Garnier J, Thorel L and Thétiot N (2003), "Cyclic Loading Effect on Pile *p-y* Curves: Centrifuge Modelling," *Foundations: Innovations, observations, Design and Practice, ICE*, London, Thomas Telford, 767−775.

Rosquoët F, Garnier J, Thorel L and Canepa Y (2004), "Horizontal Cyclic Loading of Piles Installed in Sand: Study of the Pile Head Displacement and Maximum Bending Moment," *Proceedings of the International Conference on Cyclic Behavior of Soils and Liquefaction Phenomena*, Bochum, T. Triantafyllidis (Ed.), Taylor & Francis, 363−368.

Schofield AN (1980), "Cambridge Geotechnical Centrifuge Operations," G*eotechnique,* **25**(4): 743−761.

Schofield AN (1981), "Dynamic and Earthquake Geotechnical Centrifuge Modelling," *Proceedings of the International Conference on Recent Advances in Geotechnical Earthquake Engineering and Soil Dynamics,* S. Prakash Foundation, 1081−1100.

Stevens JB and Audibert JME (1979), "Re-examination of *p−y* Curve Formulations," *Proceedings of the 11th Offshore Technology Conference,* Paper No OTC 3402, 397−403.

Tabesh A and Poulos HG (2001), "The Effects of Soil Yielding on Seismic Response of Single Piles," *Soils and Foundations,* **41**(3): 1−16.

Trochanis A, Bielak J and Christiano P (1991), "Three-dimensional Nonlinear Study of Piles," *Journal of the Geotechnical Engineering,* ASCE*,* **117:** GT3, 429-47.

Trochanis A, Bielak J and Christiano P (1994), "Simplified Model for Analysis of One or Two Piles,"

Journal of Engineering Mechanics, ASCE, **120**: 308-29.

Wakai A, Gose Sh and Ugai K (1999), "3-D Elasto-plastic Finite Element Analyses of Pile Foundations Subjected to Lateral Loading," *Soils & Foundations*, **39**(1): 97−111.

Wen YK (1976), "Method for Random Vibration of Hysteretic Systems," *Journal of Engineering Mechanics,* ASCE, **102**: 249-263.

Whitman RV, Lambe PC and Kutter BL (1981), "Initial Results from a Stacked Ring Apparatus for Simulation of a Soil Profile," *International Conference on Recent Advances in Geotechnical Earthquake Engineering and Soil Dynamics,* S. Prakash Foundation, **III**: 1105−1113.

Wu B, Broms B and Choa V (1998), "Design of Laterally Loaded Piles in Cohesive Soils Using *p*−*y* curves," *Soils and Foundations*, **38**(2): 17−26.

Yegian M and Wright SG (1973), "Lateral Soil Resistance-displacement Relationships for Pile Foundations in Soft Clays," *Proceedings of the 5th Offshore Technology Conference,* Paper No. OTC 1893, II−663−II−676.